Original Article

Differential diagnostic performance of PET/CT in adult-onset still's disease and lymphoma: a retrospective pilot study

Liyan Wan[1,2#], Yuting Gao[3#], Chendie Yang[4], Jieyu Gu[1], Tingting Liu[1], Qiongyi Hu[1], Zihan Tang[1], Jialin Teng[1], Honglei Liu[1], Xiaobing Cheng[1], Junna Ye[1], Yutong Su[1], Yi Shi[5], Xinyun Huang[3], Chengde Yang[1], Biao Li[3], Hui Shi[1], Min Zhang[3]

[1]Department of Rheumatology and Immunology, Ruijin Hospital, Shanghai Jiao Tong University School of Medicine, Shanghai, China; [2]Department of Rheumatology, The First Affiliated Hospital, Zhejiang University School of Medicine, Hangzhou, China; [3]Department of Nuclear Medicine, Ruijin Hospital, Shanghai Jiao Tong University School of Medicine, Shanghai, China; [4]Department of Cardiology, Ruijin Hospital, Shanghai Jiao Tong University School of Medicine, Shanghai, China; [5]Bio-X Institutes, School of Life Science and Biotechnology, Shanghai Jiao Tong University, Shanghai, China

Contributions: (I) Conception and design: M Zhang, Chengde Yang, H Shi; (II) Administrative support: B Li, Chengde Yang; (III) Provision of study materials or patients: L Wan, Chendie Yang, J Gu, T Liu, Q Hu, J Teng, H Liu, X Cheng, J Ye, Y Su, Chengde Yang; (IV) Collection and assembly of data: L Wan, Chendie Yang, J Gu, T Liu, Q Hu, J Teng, H Liu, X Cheng, J Ye, Y Su, Chengde Yang; (V) Data analysis and interpretation: M Zhang, B Li, X Huang, Y Gao, L Wan, Y Shi, J Gu; (VI) Manuscript writing: All authors; (VII) Final approval of manuscript: All authors.

[#]These authors contributed equally to this work and should be considered as co-first authors.

Correspondence to: Min Zhang, MD, PhD. Department of Nuclear Medicine, Ruijin Hospital, Shanghai Jiao Tong University School of Medicine, 197 Ruijin 2nd Road, Shanghai 200025, China. Email: zm11518@rjh.com.cn; Hui Shi, MD, PhD. Department of Rheumatology and Immunology, Ruijin Hospital, Shanghai Jiao Tong University School of Medicine, Shanghai 200025, China. Email: shihui_sjtu@sina.com.

Background: Adult-onset still's disease (AOSD) and lymphoma are the common causes of fever of unknown origin (FUO) and show some similar clinical symptoms. This study aimed to establish a reliable and easy-to-used scoring model based on clinical information, laboratory characteristics and ^{18}F-fluorodeoxyglucose positron emission tomography/computer tomography (^{18}F-FDG PET/CT) images for the differential diagnosis of these two diseases.

Methods: A development cohort including 70 AOSD and 37 lymphoma patients was used to establish a scoring model based on the features of PET/CT images. The scoring model was then validated in a validation cohort of 15 AOSD and 12 lymphoma patients. The features of involved bone marrow, spleen, lymph nodes, and other organs or tissues displayed on PET/CT images were compared. Multiple logistics regression and decision tree analysis were used to establish the scoring model.

Results: Four features that could significantly differentiate these two diseases were selected to establish a scoring model discriminating AOSD from lymphoma, including (I) white blood cell (WBC) count $\leq 10\times10^9$/L (1 point); (II) ferritin ≤ upper limit of normal (ULN) (1 point); (III) no abnormal bone marrow metabolism (1 point); (IV) total lesion glycolysis$_{total}$ (TLG_{total}) >9.0 (1 point). After decision tree analysis, it showed that a score ≤1 indicates AOSD. A score ≥3 strongly suggested lymphoma, with a sensitivity of 81.1% and specificity of 90.0% in the development cohort, and a sensitivity of 58.3% and specificity of 100% in the validation cohort.

Conclusions: Our scoring model showed good diagnosis performance in distinguishing AOSD from lymphoma.

Keywords: ^{18}F-fluorodeoxyglucose positron emission tomography/computer tomography; adult-onset still's disease (AOSD); lymphoma; differential diagnosis; autoinflammatory disease

Submitted Mar 16, 2022. Accepted for publication Oct 01, 2022. Published online Nov 02, 2022.
doi: 10.21037/qims-22-246
View this article at: https://dx.doi.org/10.21037/qims-22-246

Introduction

Fever of unknown origin (FUO) is a prolonged febrile illness without an established etiology, including an arrays of diseases with unspecific symptoms (1). Adult-onset still's disease (AOSD), a systemic autoinflammatory disorder (2), is one of the common causes of FUO (1). AOSD is typically characterized by spiking fever, transient rash, lymphadenopathy, and hepatosplenomegaly. The diagnosis of AOSD can be established only after the exclusion of infections, other autoimmune diseases, and neoplasms (3).

Lymphoma is also a well-known malignant cause of FUO (4). The initial symptoms of lymphoma are lymphadenopathy and fever, accompanied by night sweat, weight loss and splenomegaly (5), which can mimic AOSD because of their similar clinical symptoms (6-8). The significant differences of the treatment strategies and prognosis between AOSD and lymphoma necessitate a reliable differential diagnostic method. Histopathological examination of lymph node biopsy is the standard procedure to diagnose lymphoma, but under the guidance of conventional imaging (CT or ultrasound), some false negative still exist (9,10), while invasive procedure also brings anxiety to the patients (11).

^{18}F-fluorodeoxyglucose positron emission tomography/computer tomography (^{18}F-FDG PET/CT) is a noninvasive whole-body imaging tool to detect the metabolic abnormalities of glucose, which has been widely used as a first-line imaging exam in the guidance of biopsy, initial staging, therapeutic assessment, and the detection of relapse of lymphoma (12-14). Meanwhile, ^{18}F-FDG PET/CT plays an essential role in the etiological diagnosis of FUO (1,4,15-17). Moreover, previous studies have revealed the value of ^{18}F-FDG PET/CT in the assessment of organ involvement in AOSD (18-21). Our previous study suggested that PET/CT could act as an early detective tool to evaluate the disease severity and predict the occurrence of macrophage activation syndrome in patients with AOSD (22). We hypothesized that there could be different whole-body imaging patterns between AOSD and lymphoma on ^{18}F-FDG PET/CT images, which may help to identify the patients more likely with AOSD than those with lymphoma for medical decision-making and treatment selection.

In the present study, we compared ^{18}F-FDG PET/CT image features between patients with AOSD and those with lymphoma who both visited our hospital due to fever, screened out the specific image features, and finally developed an easy-to-use scoring model based on clinical information, laboratory characteristics and ^{18}F-FDG PET/CT images for differentiating these two diseases. We present the following article in accordance with the STARD reporting checklist (available at https://qims.amegroups.com/article/view/10.21037/qims-22-246/rc).

Methods

Identification and selection of patients

This study was conducted in accordance with the Declaration of Helsinki (as revised in 2013) and was approved by the Ethics Committee of Ruijin Hospital, Shanghai Jiao Tong University School of Medicine. As a retrospective study, this study was exempt from the informed consent. We sought out all the patients with fever who underwent ^{18}F-FDG PET/CT in Ruijin hospital, Shanghai Jiao Tong University School of Medicine between July 1, 2016 and January 31, 2019, of whom 322 patients fulfilled the definition of FUO, as a febrile illness with body temperatures >38.3 ℃ lasting over at least 3 weeks without achieving diagnosis after thorough history taking, physical examination and standard diagnostic procedures (1). Among these patients, 70 patients were diagnosed with AOSD. Two senior rheumatologists reviewed and agreed upon the diagnosis of AOSD in 70 patients based on a combination of clinical, laboratory, and radiological findings, as well as response to treatment and follow-up with the reference of the Yamaguchi's criteria (23). Among the patients pathologically diagnosed as lymphoma by biopsy, we excluded the patients only with extranodal involvement, whose radiological findings were significantly different from AOSD. Finally, 37 patients with lymphoma were enrolled in the development cohort. Another 15 patients with AOSD and 12 patients with lymphoma who visited in our hospital due to fever and underwent ^{18}F-FDG PET/CT scan from February 1, 2019 to September 30, 2019, were consecutively recruited in the validation cohort

(Figure S1). All recruited patients were treatment naive while they underwent the ^{18}F-FDG PET/CT scan. We calculated the power of the Wald tests of the parameters being equal to 0 (null hypothesis) under a significance level of 5% (two-sided). So, the final study size in this manuscript ensures that a sufficient amount of precision is reached.

All laboratory results, including white blood cell (WBC) counts, percentage of neutrophils (N%), erythrocyte sedimentation rate (ESR), C-reactive protein (CRP), ferritin and lactate dehydrogenase (LDH), were recorded as those most recent to PET/CT scan. The maximum interval between laboratory results and PET/CT scan was 2 weeks, while average interval was 4.5±2.1 days.

PET/CT imaging

The integrated ^{18}F-FDG PET/CT study was performed on the GE Discovery VCT64 system (GE healthcare). All patients fasted for at least 6 hours and confirmed the blood glucose level to be less than 200 mg/dL before ^{18}F-FDG administration. Approximately 50 to 70 min after the intravenous injection of 5 MBq of ^{18}F-FDG per kilogram to the patients, PET images were acquired for 3 min per bed position using 128×128 matrix size, 28 subsets, two iterations, and full-width half-maximum post-filtering the skull base to the mid-thigh. CT images were acquired using 140 kV tube voltage, 220 mA tube current, and 3.75 mm section thickness. PET images were reconstructed based on the ordered-subset expectation-maximization algorithm with photon attenuation correction from the CT data.

Image analysis

^{18}F-FDG PET/CT images were reviewed on AW workstation 4.7 (GE Healthcare) by two experienced nuclear physicians blinded to the clinical and biologic data of patients. The maximum standardized uptake value (SUV_{max}) of bone marrow was obtained from lumbar vertebrae 1–5, as a cube-shaped volume of interesting (VOI) was drawn at the level of the lumbar vertebrae 1–5, while the VOI should avoid the adjacent large blood vessels and the lower pole of the kidney. The SUV_{max} of spleen was obtained by drawing a region of interest (ROI) on splenic hilum slice. The SUV_{max} of liver was obtained by drawing a 3-cm-diameter ROI in the right lobe of liver. The abnormal hypermetabolism of bone marrow, spleen and liver were defined as SUV_{max} higher than the 95th percentile for the glucose metabolic level of them in the healthy controls (22). The abnormal hypermetabolism of lymph nodes was identified based on a visual comparison of FDG uptake between the background organ and target site. The SUV_{max} and minimal axial diameter of the hypermetabolic lymph node were recorded. Because AOSD-affected lymph nodes were non-neoplastic, the metabolic volume of involved lymph nodes in both patients with lymphoma and those with AOSD was uniformly named as metabolic lesion volume (MLV) instead of conventionally used metabolic tumor volume (MTV) in this study (24). MLV was automatically delineated using a threshold of 40% of the SUV_{max}. Total lesion glycolysis (TLG) of hypermetabolic lymph nodes were also measured. The summed MLV (MLV_{total}) and TLG (TLG_{total}) in all hypermetabolic lymph nodes were calculated to evaluate the whole-body disease burden. Because of the irregular shape of the bone marrow and spleen, it was difficult to obtain VOIs completely covering either organ where the MLV and TLG could not be measured. Splenomegaly and the involved extranodal organs and tissues with abnormal ^{18}F-FDG uptake, such as tonsils, salivary glands, ankle, were also recorded.

Statistical analysis

Categorical variables are presented as number (%) and continuous variables are presented as mean ± standard deviation (SD) or median, [first quartile (Q1), third quartile (Q3)]. The SUV_{max} of the most hypermetabolic lymph node were used as SUV_{max} of lymph node in data analysis. Between-group comparisons were performed with the Chi-Square test, Fisher's exact, and *t*-test, as appropriate. Laboratory indicators were converted to categorical data using clinical cut-off value. Continuous ^{18}F-FDG PET/CT imaging data were first converted to categorical data by utilizing the receiver operating characteristic (ROC) curves to choose the best probabilistic cut-off values (25) or 95th percentile in healthy controls (22). All the variables were assessed using logistic regression or Firth logistic regression (26). After univariate analysis, those variables with P value <0.01 were further enrolled into the multivariate logistics regression with the forward conditional mode. In accordance with the study of Sciascia *et al.*, each variable was proportionally assigned a weighted value according to the magnitude of the logistic equation's coefficients (27). The Chi-Squared Automatic Interaction Detection (CHAID) approach was used to grow the tree. Due to the class imbalance in our develop cohort, a higher weight for the lymphoma was specified in growing the

Table 1 Characteristics of patients in the development and validation cohorts

Characteristics	Development cohort (n=107)	Validation cohort (n=27)	P
Demographics			
Sex			0.310
Female	78 (72.9)	17 (63.0)	
Male	29 (27.1)	10 (37.0)	
Age (years)	43.19±17.07	42.78±17.34	0.960
Diagnosis			0.342
AOSD	70 (65.4)	15 (55.6)	
Lymphoma	37 (34.6)	12 (44.4)	
B cell lymphoma	19	8	
T/NK cell lymphoma	16	2	
Hodgkin lymphoma	2	2	
Disease duration (weeks)	3 (3, 4)	3 (3, 4)	0.565
Clinical manifestation			
Fever >39 ℃	62 (57.9)	17 (63.0)	0.669
Lymphadenopathy	83 (77.6)	16 (59.3)	0.053
Splenomegaly	49 (45.8)	13 (48.1)	0.827
Arthralgia	61 (57.0)	13 (48.1)	0.408
Pharyngalgia	53 (49.5)	13 (48.1)	0.898
Rash	65 (60.7)	15 (55.6)	0.623
Laboratory parameters			
WBC ($\times 10^9$/L)	8.7 (5.8, 14.7)	9.6 (5.0, 12.8)	0.655
Neutrophils (%)	78.0 (67.9, 85.6)	78.0 (68.7, 86.0)	0.854
ESR (mm/h)	59 (28, 87)	67 (38, 80)	0.696
CRP (mg/L)	62.1 (18.7, 133.5)	81.4 (47.7, 151.0)	0.275
Serum ferritin (ng/mL)	1,499 (437, 1,500)	1,735 (655, 7,743)	0.027
LDH (IU/L)	337 (215, 633)	450 (277, 700)	0.140

Categorical variables are presented as number (%) or number and continuous variables are presented as mean ± SD or median (Q1, Q3). AOSD, adult-onset still's disease; WBC, white blood cell; ESR, erythrocyte sedimentation rate; CRP, C-reactive protein; LDH, lactate dehydrogenase; SD, standard deviation; Q1, first quartile; Q3, third quartile.

decision tree. The confusion matrix, positive predictive value (PPV), and negative predictive value (NPV), and areas under the curves (AUCs) from ROC analysis were analyzed to determine the diagnostic performance of the imaging features and the scoring model. A P value less than 0.05 (two-tailed) was considered to be statistically significant. As an estimate of effect size and variability, we have reported the odds ratio (OR) with a 95% confidence interval (CI). All statistical analyses were performed with MedCalc (version 9.2.0), SPSS (version 23.0) and R (version 3.6.2) software packages.

Results

Patients' characteristics

A total of 107 patients were included in the development cohort and 27 patients in the validation cohort, and their characteristics are shown in *Table 1*. There was no

Table 2 Comparison of clinical characteristics between patients with AOSD and those with lymphoma in the development cohort

Characteristics	AOSD (n=70)	Lymphoma (n=37)	P
Demographics			
Sex			<0.001
Female	59 (84.3)	19 (51.4)	
Male	11 (15.7)	18 (48.6)	
Age (years)	39.2±15.5	50.8±17.5	0.001
Disease duration (weeks)	3 (3, 4)	3 (3, 6)	0.241
Clinical manifestation			
Fever >39 ℃	55 (78.6)	7 (18.9)	<0.001
Lymphadenopathy	51 (72.9)	32 (86.5)	0.108
Splenomegaly	26 (37.1)	23 (62.2)	0.013
Arthralgia	58 (82.9)	3 (8.1)	<0.001
Pharyngalgia	48 (68.6)	5 (13.5)	<0.001
Rash	62 (88.6)	3 (8.1)	<0.001
Laboratory parameters			
WBC ($\times 10^9$/L)	11.0 (7.8, 17.6)	5.7 (2.6, 8.6)	<0.001
Neutrophils (%)	81.4 (75.2, 87.8)	66.8 (52.0, 77.2)	<0.001
ESR (mm/h)	70 (36, 86)	30 (15, 94)	0.012
CRP (mg/L)	70.0 (31.2, 137.2)	30.9 (11.0, 103.6)	0.023
Serum ferritin (ng/mL)	1,500 (998, 2,093)	555 (239, 1,088)	<0.001
LDH (IU/L)	432 (258, 666)	286 (180, 488)	0.057

Categorical variables are presented as number (%) and continuous variables are presented as mean ± SD or median (Q1, Q3). AOSD, adult-onset still's disease; WBC, white blood cell; ESR, erythrocyte sedimentation rate; CRP, C-reactive protein; LDH, lactate dehydrogenase; SD, standard deviation; Q1, first quartile; Q3, third quartile.

significant difference in age, gender, diagnosis and clinical manifestations between development cohort and validation cohort.

Table 2 shows a comparison of clinical characteristics between patients with AOSD and those with lymphoma in the development cohort, while the characteristics of patients in the validation cohort were displayed in Table S1. The proportion of female in patients with AOSD was higher than that of patients with lymphoma (P<0.001) in the development cohort, while there was no significant gender difference in the validation cohort. Patients with AOSD were significantly younger than those with lymphoma in both development (39.2±15.5 and 50.8±17.5, P=0.001) and validation (33.5±11.9 and 54.3±16.3, P=0.001) cohorts. The prevalence of fever >39 ℃, arthralgia, pharyngalgia and rash was more frequent in the patients with AOSD than in the lymphoma group, while splenomegaly occurred more frequently in the patients with lymphoma (37.1% *vs.* 62.2%, P=0.013). There was no significant difference in the prevalence of lymphadenopathy between the two diseases. Laboratory inflammatory markers, including WBC, neutrophils, CRP, ESR, and serum ferritin of patients with AOSD were dramatically higher than those of patients with lymphoma.

Comparison of ^{18}F-FDG PET/CT imaging features between AOSD and lymphoma

In the development cohort, abnormally increased ^{18}F-FDG uptake pattern of different organs and tissues were compared between AOSD and lymphoma, as shown in *Table 3*. The accumulation of ^{18}F-FDG was significantly

Table 3 Comparison of ^{18}F-FDG PET/CT imaging features between AOSD and lymphoma in the development cohort

Features	AOSD (n=70)	Lymphoma (n=37)	P
Bone marrow			
SUV_{max}	5.2 (4.3, 6.1)	4.0 (3.4, 4.5)	<0.001
Hypermetabolism	43 (61.4)	6 (16.2)	<0.001
Spleen			
SUV_{max}	3.8 (3.1, 4.4)	3.6 (2.7, 5.6)	0.649
Hypermetabolism	56 (80.0)	21 (56.8)	0.011
Liver			
SUV_{max}	3.2 (2.8, 3.5)	3.4 (2.7, 4.0)	0.414
Hypermetabolism	7 (10.0)	9 (24.3)	0.048
Lymph node			
SUV_{max}	4.9 (2.3, 8.0)	8.8 (3.6, 16.1)	0.003
Hypermetabolism	70 (100.0)	36 (97.3)	0.346
MLV_{total} (cm^3)	11.44 (1.57, 39.33)	57.78 (6.95, 128.64)	<0.001
TLG_{total}	28.1 (2.8, 142.4)	207.1 (25.6, 889.2)	<0.001
Other hypermetabolic tissues			
Pharynx	18 (25.7)	9 (24.3)	0.394
Salivary glands	9 (12.9)	1 (2.7)	0.213
Gastrointestinal tract	0	4 (10.8)	<0.001
Ankles and muscles	8 (11.4)	1 (2.7)	0.271
Others[a]	0	13 (35.1)	<0.001

Categorical variables are presented as number (%) and continuous variables are presented as median (Q1, Q3). [a], including pancreas, breast, thyroid, adrenal gland, sinuses, subcutaneous tissue, and pulmonary involvement. ^{18}F-FDG PET/CT, ^{18}F-fluorodeoxyglucose positron emission tomography/computer tomography; AOSD, adult-onset still's disease; SUV_{max}, maximum standardized uptake value; MLV, metabolic lesion volume; TLG, total lesion glycolysis; Q1, first quartile; Q3, third quartile.

higher in bone marrow in patients with AOSD (median: 5.2; Q1, Q3: 4.3, 6.1) than those of patients with lymphoma (median: 4.0; Q1, Q3: 3.4, 4.5; P<0.001). Spleen hypermetabolism occurred more frequently in the patients with AOSD than those with lymphoma (80.0% *vs.* 56.8%, P=0.011). In contrast, liver hypermetabolism occurred more frequently in the patients with lymphoma than those with AOSD (10.0% *vs.* 24.3%, P=0.048). Patients with AOSD and those with lymphoma had comparable prevalence of abnormal hypermetabolic lymph nodes (100.0% *vs.* 97.3%, P=0.346). However, the median SUV_{max} of lymphadenopathy in patients with AOSD was still lower than that in patients with lymphoma (4.9 *vs.* 8.8, P=0.003). The MLV_{total} (P<0.001) and TLG_{total} (P<0.001) in patients with AOSD were significantly lower than those in patients with lymphoma. On the contrary, there was significant difference in the percentage of involved gastrointestinal tract between AOSD and lymphoma (0 *vs.* 10.8%, P<0.001). In addition, some other involved extranodal tissues in patients with lymphoma but not in patients with AOSD on PET/CT images, such as pancreas, breast, nasopharynx, thyroid, adrenal gland, and pulmonary were found. Representative PET/CT images of abnormal hypermetabolic distributions in one patient with AOSD and one patient with lymphoma were depicted in *Figures 1,2*.

Establishment of the scoring model for differentiating AOSD from lymphoma

Using the clinical cut-off values, 95th percentile in

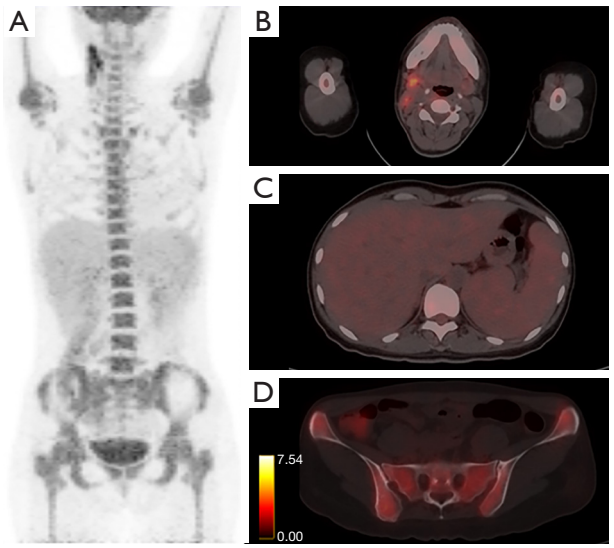

Figure 1 Whole-body PET image (A), and axial hybrid PET/CT images of axillary LNs (B), liver and spleen (C), and spine (D) from a 37-year-old female patient with fever, sore throat, skin rash, lymphadenopathy, and arthralgia. Her laboratory results were listed as WBC count 10.6×10^9/L, neutrophil percentage 85.2%, ESR 105 mm/h, CRP 135 mg/L, and ferritin 349 ng/mL. Serological workup for rheumatoid factor and anti-nuclear antibodies was negative. It showed ^{18}F-FDG uptake by right submandibular and neck LNs (SUV_{max}, 2.2–6.1; diameter, 0.8–1.4 cm), spleen (SUV_{max}, 2.2), liver (SUV_{max}, 2.5), and bone marrow (SUV_{max}, 5.0). The TLG_{total} of LNs was 58.1, and MLV_{total} of LNs was 20.05. She was diagnosed with AOSD after exclusion of malignancy and infection. After receiving methylprednisolone 80 mg daily, her body temperature turned normal and rash and arthralgia were relieved. Her score is 0 in our model. PET, positron emission tomography; CT, computer tomography; LNs, lymph nodes; WBC, white blood cell; ESR, erythrocyte sedimentation rate; CRP, C-reactive protein; ^{18}F-FDG, ^{18}F-fluorodeoxyglucose; SUV_{max}, maximum standardized uptake value; TLG, total lesion glycolysis; MLV, metabolic lesion volume; AOSD, adult-onset still's disease.

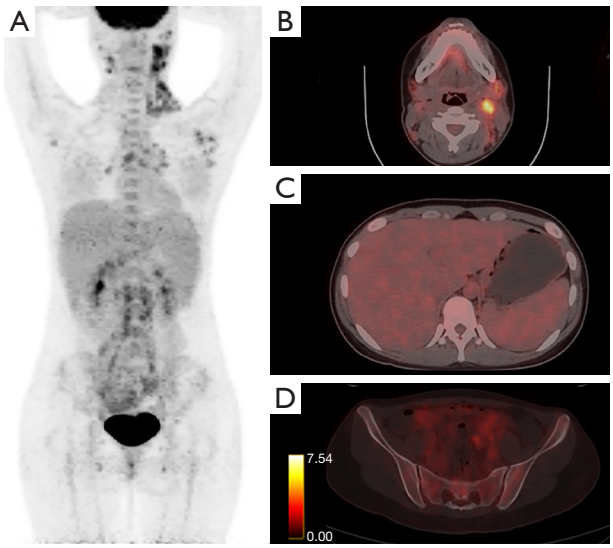

Figure 2 Whole-body PET image (A), and axial hybrid PET/CT images of left submandibular lymph node (B), liver and spleen (C), and pelvis bone (D) from a 19-year-old female patient with fever, lymphadenopathy, and arthralgia. Her laboratory results were listed as WBC count 7.4×10^9/L, neutrophil percentage 77.8%, ESR 53 mm/h, CRP 153 mg/L, LDH 314 IU/L, and ferritin 132 ng/mL. It showed ^{18}F-FDG uptake by left submandibular, cervical, subaxilliary, mediastinal and abdominal LNs (SUV_{max}, 2.5–9.8; diameter, 0.8–1.5 cm), mediastinum LNs (SUV_{max}, 7.4), spleen (SUV_{max}, 4.2), liver (SUV_{max}, 3.3), and bone marrow (SUV_{max}, 3.9). The TLG_{total} of LNs was 884.2, and MLV_{total} of LNs was 292.15. After biopsy of lymph node, she was diagnoses with anaplastic large-cell lymphoma. Her score is 4 in our model. PET, positron emission tomography; CT, computer tomography; WBC, white blood cell; ESR, erythrocyte sedimentation rate; CRP, C-reactive protein; LDH, lactate dehydrogenase; ^{18}F-FDG, ^{18}F-fluorodeoxyglucose; LNs, lymph nodes; SUV_{max}, maximum standardized uptake value; TLG, total lesion glycolysis; MLV, metabolic lesion volume.

healthy controls or the ROC curves analysis to choose the best probabilistic cut-off values, all the continuous data were converted to categorical parameters (Table S2). All clinical information, laboratory biomarkers and PET/CT parameters were included in univariate logistic regression analysis (Table S3). Furthermore, after multivariate logistics regression (*Table 4*), four features which can discriminate these two diseases effectively were screened out, and finally enrolled in the scoring model: (I) WBC count $\leq10\times10^9$/L (1 point); (II) ferritin ≤ upper limit of normal (ULN) (1 point); (III) no abnormal bone marrow metabolism (1 point); (IV) TLG_{total} >9.0 (1 point).

Diagnostic performance of the scoring model in the development and validation cohorts

Figure 3 showed the analysis of decision tree using the scoring model in the development cohort. As a result, the patients with 1 or fewer points totally were correctly classified as AOSD (n=34), and those with scores higher

than or equal to 3 points were more likely to have lymphoma (30/37, 81.1%). The patients with 2 points (29 with AOSD, 7 with lymphoma) was classified as uncertain disease, which required a further evaluation. In the validation sample, all the 11 patients with 1 or fewer point had AOSD; of the 9 patients with a score of 2, 4 had AOSD and 5 had lymphoma; all the 7 patients with 3 or 4 points had lymphoma. The AUCs of the scoring model in the development and validation cohorts were 0.855 (95% CI: 0.771–0.940) and 0.792 (95% CI: 0.603–0.980), respectively (*Table 5*).

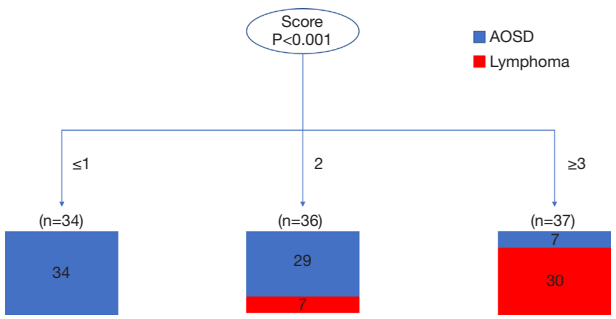

Figure 3 Decision tree model for distinguishing lymphoma from AOSD in the development cohort. AOSD, adult-onset still's disease.

Discussion

Although the demography (28,29), clinical and hematological profile (30) often vary greatly between AOSD and lymphoma, our study showed that patients with AOSD or lymphoma whose initial symptoms were persistent fever, had overlapping clinical and laboratory characteristics, which emphasized the importance of differential diagnosis for the two diseases. Sometimes it is difficult to make a diagnosis only based on clinical symptoms or conventional radiology, while FDG PET/CT is an add-on criterion. Therefore, we developed a user-friendly and quantitative scoring model based on ^{18}F-FDG PET/CT images features accompanied with clinical information and laboratory characteristics to identify the patients more likely with AOSD rather than with lymphoma, which may direct the final examination and impact on the choice of treatment.

In our study, both SUV_{max} and hypermetabolic prevalence of bone marrow were significantly higher in patients with AOSD than those with lymphoma. The diffuse and high accumulation of ^{18}F-FDG in bone marrow may correlate to the activation of aberrant inflammatory response, inducing a variety of inflammatory cytokines and simulating myeloproliferative activity in patients with AOSD (31). On the contrary, the incidence of bone marrow

Table 4 Multivariate logistic regression models for differentiating AOSD from lymphoma

Features	P	OR	95% CI of OR	β-coefficient	Score
WBC ≤10×10^9/L	0.001	16.168	3.016–86.672	0.283	1
Ferritin ≤ ULN	0.002	28.567	3.284–248.477	0.333	1
No abnormal bone marrow metabolism	<0.001	13.272	3.442–51.175	0.305	1
TLG_{total} >9.0	0.003	23.623	2.992–186.505	0.254	1

AOSD, adult-onset still's disease; WBC, white blood cell; ULN, upper limit of normal; TLG, total lesion glycolysis; OR, odds ratio; CI, confidence interval.

Table 5 Differential diagnostic performance of the decision tree analysis

Group	AUC (95% CI)	PPV (95% CI), %	NPV (95% CI), %	True positive for lymphoma, n	False positive for lymphoma, n	True negative for lymphoma, n	False negative for lymphoma, n
Development cohort	0.855 (0.771–0.940)	81.1 (67.6–89.8)	90 (82.1–94.6)	30	7	63	7
Validation cohort	0.792 (0.603–0.980)	100 (100–100)	75 (60.6–85.4)	7	0	15	5

AUC, area under the curve; CI, confidence interval; PPV, positive predictive value; NPV, negative predictive value.

hypermetabolism in patients with lymphoma in our study was much low (16.2%). Consistent with our results, a previous study also revealed only 10% to 25% bone marrow involvement in patients with lymphoma (32). Furthermore, the glucose metabolic intensity of bone marrow in patients with lymphoma was only slightly higher or comparable to normal bone marrow metabolism level, showing a significantly different imaging pattern of bone marrow from patients with AOSD.

Patients with AOSD had lower incidence of splenomegaly, but more frequent hypermetabolism of the spleen than those with lymphoma. That is, even if without splenomegaly, patients with AOSD tended to have abnormally increased glucose metabolism, which suggested the high inflammatory activity in the spleen of AOSD patients. However, there was no difference in the glucose metabolic intensity of spleen between patients with lymphoma and AOSD, therefore which did not enter the final diagnostic model as a valid parameter.

According to this study, lymph nodes in patients with AOSD showed a lower glucose metabolic level compared to patients with lymphoma, although the SUV_{max}, MLV and TLG were different between different histological type of lymphoma, which was consistent with the analysis of lymphoma as a whole (Table S4). Previous reports showed that ^{18}F-FDG uptake level in the lymph nodes of patients with AOSD varied widely, with the SUV_{max} ranging from 2.2 to 13.9 (21), which partially overlapped with that in patients with lymphoma (33). The prevalence of lymphadenopathy seemed higher in the patients with lymphoma than patients with AOSD. Lymphadenopathy in patients with AOSD is mainly due to benign paracortical hyperplasia accompanied by vascular and immunoblastic proliferation (34), restricting the enlargement of the lymph nodes. In contrast, the size of lymph nodes in malignant proliferating lymphoma can be extraordinarily large, with a maximum diameter of 7 cm (35). Besides, no fused lymph node was observed in patients with AOSD in Dong *et al.*'s (19) and our study, while the fused lymph node is a common feature in lymphoma. As the single-voxel-based SUV_{max} cannot reflect whole-body disease burden, three-dimensional measurement parameters including MLV and TLG were used in this study. Both MLV and TLG conventionally play essential roles to diagnose the lymphoma, especially to predict the therapeutic outcomes (36-38), while their roles in the prognosis of AOSD has also been described (22). In our study, we found that whole-body disease burden evaluated by both MLV_{total} and TLG_{total} of lymph nodes in patients with lymphoma were significantly higher than those of patients with AOSD. However, assessing all FDG-uptaking lesions consumes too much time, which acquires more advanced automatic lesion segmentation algorithms based on AI computing in the future.

After screening for various clinical, laboratory, and PET/CT parameters, we developed our own scoring model for differential diagnosis and deliberately chose a model with high specificity, so that the model can diagnose AOSD more accurately in clinical practice. Our model diagnosed the patients with 1 or fewer points as AOSD, the patients with 2 points as uncertain disease and the patients with 3 or 4 points as most likely lymphoma. Concerning the patients with 1 or fewer points showing a low risk of lymphoma, there will need great caution before invasive biopsy, and the patients with 2 or more points should have a further examination. Among the 36 patients in the "grey zone", there were 29 patients with AOSD and 7 patients with lymphoma. Most of patients with AOSD were unclassified because of non-evaluated WBC level and increased TLG_{total}, while most of patients with lymphoma were unclassified because of high level of ferritin and bone marrow hypermetabolism (Table S5). It seemed that the lymphoma patients with high levels of inflammation were more likely to be misclassified.

There are still some limitations in this study. (I) The enrolled patients are highly selected, then our model cannot be extrapolated to other diseases that need to be differentiated from AOSD, such as infections, IgG4-RD, sarcoidosis, and solid cancers. Nevertheless, this work represents a step forward in the differential diagnosis of AOSD by applying the PET/CT scanning. (II) The numbers of recruited patients are small leading to the possibility of model overfitting. This study was a pilot study at a single center, and more high evidence studies are needed to verify the reliability of the PET/CT parameters and our model for differentiating AOSD from lymphoma. Also, further studies are necessary to understand whether this score can be useful to discriminate other disorders that may mimic AOSD.

Conclusions

Above all, a scoring model including WBC count, ferritin, metabolism of bone marrow and TLG_{total} of lymph nodes was finally developed. In the validation cohort, the model correctly classified all 15 cases with AOSD, and showed a good diagnostic performance with high specificity and PPV

for differentiating AOSD from lymphoma. Concerning the patients with 1 or fewer points showing a low risk of lymphoma, rheumatologists can better identify patients with AOSD, and reduce unnecessary invasive biopsy in around 60% of patients with AOSD.

Acknowledgments

Funding: This study was supported by grants from Shanghai Jiao Tong University Medicine & Engineering Interdisciplinary Funding (No. YG2017QN58 to H Shi, No. YG2017MS61 to M Zhang), Shanghai Municipal Key Clinical Specialty (No. shslczdzk03403 to B Li), and Shanghai "Medical Garden Rising Star" Youth Medical Talent Training Funding Program to Min Zhang.

Footnote

Reporting Checklist: The authors have completed the STARD reporting checklist. Available at https://qims.amegroups.com/article/view/10.21037/qims-22-246/rc

Conflicts of Interest: All authors have completed the ICMJE uniform disclosure form (available at https://qims.amegroups.com/article/view/10.21037/qims-22-246/coif). The authors have no conflicts of interest to declare.

Ethical Statement: The authors are accountable for all aspects of the work in ensuring that questions related to the accuracy or integrity of any part of the work are appropriately investigated and resolved. This study was conducted in accordance with the Declaration of Helsinki (as revised in 2013). The study was approved by the Ethics Committee of Ruijin Hospital, Shanghai Jiao Tong University School of Medicine. As a retrospective study, this study was exempt from the informed consent.

References

1. Schönau V, Vogel K, Englbrecht M, Wacker J, Schmidt D, Manger B, Kuwert T, Schett G. The value of 18F-FDG-PET/CT in identifying the cause of fever of unknown origin (FUO) and inflammation of unknown origin (IUO): data from a prospective study. Ann Rheum Dis 2018;77:70-7.
2. Giacomelli R, Ruscitti P, Shoenfeld Y. A comprehensive review on adult onset Still's disease. J Autoimmun 2018;93:24-36.
3. Gopalarathinam R, Orlowsky E, Kesavalu R, Yelaminchili S. Adult Onset Still's Disease: A Review on Diagnostic Workup and Treatment Options. Case Rep Rheumatol 2016;2016:6502373.
4. Wang Q, Li YM, Li Y, Hua FC, Wang QS, Zhang XL, Cheng C, Wu H, Yao ZM, Zhang WF, Hou QY, Miao WB, Wang XM. 18F-FDGPET/CT in fever of unknown origin and inflammation of unknown origin: a Chinese multi-center study. Eur J Nucl Med Mol Imaging 2019;46:159-65.
5. Shankland KR, Armitage JO, Hancock BW. Non-Hodgkin lymphoma. Lancet 2012;380:848-57.
6. Dudziec E, Pawlak-Buś K, Leszczyński P. Adult-onset Still's disease as a mask of Hodgkin lymphoma. Reumatologia 2015;53:106-10.
7. Soy M, Ergin M, Paydas S. Lymphadenopathy in adult-onset Still's disease mimicking peripheral T-cell lymphoma. Clin Rheumatol 2004;23:81-2.
8. Otrock ZK, Hatoum HA, Uthman IW, Taher AT, Saab S, Shamseddine AI. Non-Hodgkin's lymphoma in a woman with adult-onset Still's disease: a case report. J Med Case Rep 2008;2:73.
9. Picardi M, Gennarelli N, Ciancia R, De Renzo A, Gargiulo G, Ciancia G, Sparano L, Zeppa P, Martinelli V, Pettinato G, Lobello R, Pane F, Rotoli B. Randomized comparison of power Doppler ultrasound-directed excisional biopsy with standard excisional biopsy for the characterization of lymphadenopathies in patients with suspected lymphoma. J Clin Oncol 2004;22:3733-40.
10. Pugliese N, Di Perna M, Cozzolino I, Ciancia G, Pettinato G, Zeppa P, Varone V, Masone S, Cerchione C, Della Pepa R, Simeone L, Giordano C, Martinelli V, Salvatore C, Pane F, Picardi M. Randomized comparison of power Doppler ultrasonography-guided core-needle biopsy with open surgical biopsy for the characterization of lymphadenopathies in patients with suspected lymphoma. Ann Hematol 2017;96:627-37.

11. Matasar MJ, Zelenetz AD. Overview of lymphoma diagnosis and management. Radiol Clin North Am 2008;46:175-98, vii.
12. Younes A, Hilden P, Coiffier B, Hagenbeek A, Salles G, Wilson W, et al. International Working Group consensus response evaluation criteria in lymphoma (RECIL 2017). Ann Oncol 2017;28:1436-47.
13. Cheson BD, Fisher RI, Barrington SF, Cavalli F, Schwartz LH, Zucca E, et al. Recommendations for initial evaluation, staging, and response assessment of Hodgkin and non-Hodgkin lymphoma: the Lugano classification. J Clin Oncol 2014;32:3059-68.
14. Chaganti S, Illidge T, Barrington S, Mckay P, Linton K, Cwynarski K, McMillan A, Davies A, Stern S, Peggs K; British Committee for Standards in Haematology. Guidelines for the management of diffuse large B-cell lymphoma. Br J Haematol 2016;174:43-56.
15. Meller J, Sahlmann CO, Scheel AK. 18F-FDG PET and PET/CT in fever of unknown origin. J Nucl Med 2007;48:35-45.
16. Kouijzer IJ, Bleeker-Rovers CP, Oyen WJ. FDG-PET in fever of unknown origin. Semin Nucl Med 2013;43:333-9.
17. Tokmak H, Ergonul O, Demirkol O, Cetiner M, Ferhanoglu B. Diagnostic contribution of (18)F-FDG-PET/CT in fever of unknown origin. Int J Infect Dis 2014;19:53-8.
18. Yamashita H, Kubota K, Takahashi Y, Minamimoto R, Morooka M, Kaneko H, Kano T, Mimori A. Clinical value of ^{18}F-fluoro-dexoxyglucose positron emission tomography/computed tomography in patients with adult-onset Still's disease: a seven-case series and review of the literature. Mod Rheumatol 2014;24:645-50.
19. Dong MJ, Wang CQ, Zhao K, Wang GL, Sun ML, Liu ZF, Xu L. 18F-FDG PET/CT in patients with adult-onset Still's disease. Clin Rheumatol 2015;34:2047-56.
20. An YS, Suh CH, Jung JY, Cho H, Kim HA. The role of 18F-fluorodeoxyglucose positron emission tomography in the assessment of disease activity of adult-onset Still's disease. Korean J Intern Med 2017;32:1082-9.
21. Jiang L, Xiu Y, Gu T, Dong C, Wu B, Shi H. Imaging characteristics of adult onset Still's disease demonstrated with 18F-FDG PET/CT. Mol Med Rep 2017;16:3680-6.
22. Wan L, Gao Y, Gu J, Chi H, Wang Z, Hu Q, Jia J, Liu T, Li B, Teng J, Liu H, Cheng X, Ye J, Su Y, Yang C, Shi H, Zhang M. Total metabolic lesion volume of lymph nodes measured by 18F-FDG PET/CT: a new predictor of macrophage activation syndrome in adult-onset Still's disease. Arthritis Res Ther 2021;23:97.
23. Yamaguchi M, Ohta A, Tsunematsu T, Kasukawa R, Mizushima Y, Kashiwagi H, Kashiwazaki S, Tanimoto K, Matsumoto Y, Ota T. Preliminary criteria for classification of adult Still's disease. J Rheumatol 1992;19:424-30.
24. Berti A, Della-Torre E, Gallivanone F, Canevari C, Milani R, Lanzillotta M, Campochiaro C, Ramirez GA, Bozzalla Cassione E, Bozzolo E, Pedica F, Castiglioni I, Arcidiacono PG, Balzano G, Falconi M, Gianolli L, Dagna L. Quantitative measurement of 18F-FDG PET/CT uptake reflects the expansion of circulating plasmablasts in IgG4-related disease. Rheumatology (Oxford) 2017;56:2084-92.
25. Tripepi G, Jager KJ, Dekker FW, Zoccali C. Diagnostic methods 2: receiver operating characteristic (ROC) curves. Kidney Int 2009;76:252-6.
26. Wang X. Firth logistic regression for rare variant association tests. Front Genet 2014;5:187.
27. Sciascia S, Sanna G, Murru V, Roccatello D, Khamashta MA, Bertolaccini ML. GAPSS: the Global Anti-Phospholipid Syndrome Score. Rheumatology (Oxford) 2013;52:1397-403.
28. Morton LM, Wang SS, Devesa SS, Hartge P, Weisenburger DD, Linet MS. Lymphoma incidence patterns by WHO subtype in the United States, 1992-2001. Blood 2006;107:265-76.
29. Feist E, Mitrovic S, Fautrel B. Mechanisms, biomarkers and targets for adult-onset Still's disease. Nat Rev Rheumatol 2018;14:603-18.
30. Zeng T, Zou YQ, Wu MF, Yang CD. Clinical features and prognosis of adult-onset still's disease: 61 cases from China. J Rheumatol 2009;36:1026-31.
31. Ahn SS, Hwang SH, Jung SM, Lee SW, Park YB, Yun M, Song JJ. Evaluation of Spleen Glucose Metabolism Using 18F-FDG PET/CT in Patients with Febrile Autoimmune Disease. J Nucl Med 2017;58:507-13.
32. Sehn LH, Scott DW, Chhanabhai M, Berry B, Ruskova A, Berkahn L, Connors JM, Gascoyne RD. Impact of concordant and discordant bone marrow involvement on outcome in diffuse large B-cell lymphoma treated with R-CHOP. J Clin Oncol 2011;29:1452-7.
33. Wu X, Pertovaara H, Korkola P, Vornanen M, Eskola H, Kellokumpu-Lehtinen PL. Glucose metabolism correlated with cellular proliferation in diffuse large B-cell lymphoma. Leuk Lymphoma 2012;53:400-5.
34. Kim HA, Kwon JE, Yim H, Suh CH, Jung JY, Han JH. The pathologic findings of skin, lymph node, liver, and bone marrow in patients with adult-onset still disease: a comprehensive analysis of 40 cases. Medicine (Baltimore) 2015;94:e787.

35. Shao H, Yang ZG, Deng W, Chen J, Tang SS, Wen LY. Tuberculosis versus lymphoma in the abdominal lymph nodes: a comparative study using contrast-enhanced MRI. Eur J Radiol 2012;81:2513-7.
36. Mikhaeel NG, Smith D, Dunn JT, Phillips M, Møller H, Fields PA, Wrench D, Barrington SF. Combination of baseline metabolic tumour volume and early response on PET/CT improves progression-free survival prediction in DLBCL. Eur J Nucl Med Mol Imaging 2016;43:1209-19.
37. Ceriani L, Martelli M, Zinzani PL, Ferreri AJ, Botto B, Stelitano C, Gotti M, Cabras MG, Rigacci L, Gargantini L, Merli F, Pinotti G, Mannina D, Luminari S, Stathis A, Russo E, Cavalli F, Giovanella L, Johnson PW, Zucca E. Utility of baseline 18FDG-PET/CT functional parameters in defining prognosis of primary mediastinal (thymic) large B-cell lymphoma. Blood 2015;126:950-6.
38. Lawal IO, Nyakale NE, Harry LM, Modiselle MR, Ankrah AO, Msomi AP, Mokgoro NP, Boshomane TG, de Wiele CV, Sathekge MM. The role of F-18 FDG PET/CT in evaluating the impact of HIV infection on tumor burden and therapy outcome in patients with Hodgkin lymphoma. Eur J Nucl Med Mol Imaging 2017;44:2025-33.

Cite this article as: Wan L, Gao Y, Yang C, Gu J, Liu T, Hu Q, Tang Z, Teng J, Liu H, Cheng X, Ye J, Su Y, Shi Y, Huang X, Yang C, Li B, Shi H, Zhang M. Differential diagnostic performance of PET/CT in adult-onset still's disease and lymphoma: a retrospective pilot study. Quant Imaging Med Surg 2023;13(1):37-48. doi: 10.21037/qims-22-246

Supplementary

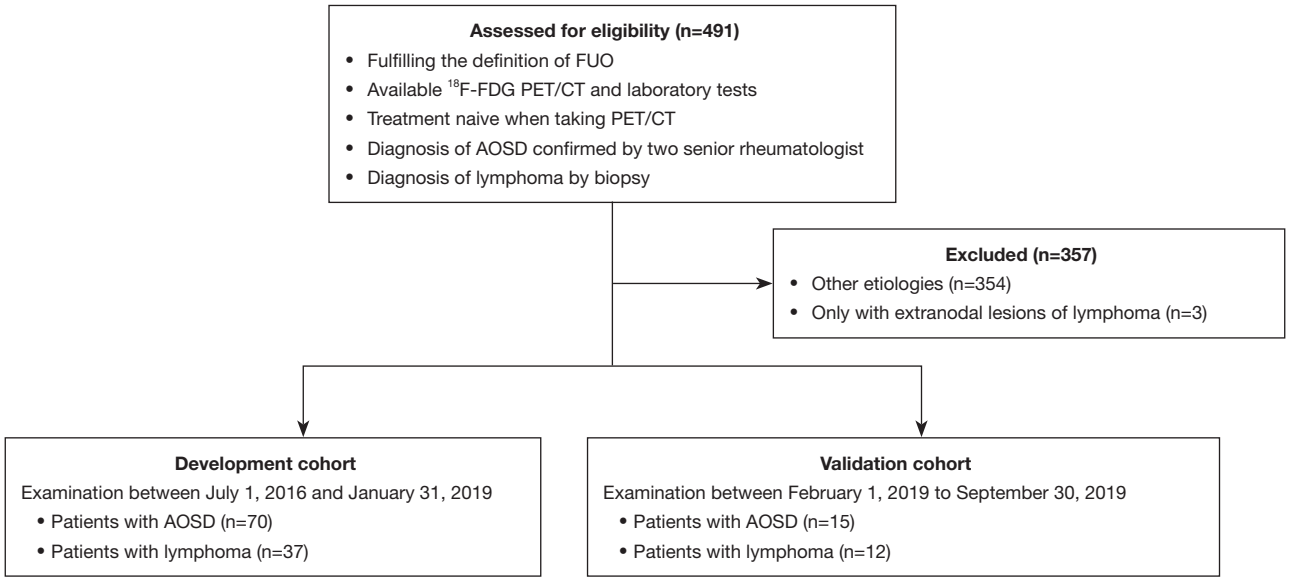

Figure S1 Flow chart of inclusions/exclusion criteria. FUO, fever of unknown origin; ^{18}F-FDG PET/CT, ^{18}F-fluorodeoxyglucose positron emission tomography/computer tomography; AOSD, adult-onset still's disease.

https://dx.doi.org/10.21037/qims-22-246

Table S1 Comparison of clinical characteristics between patients with AOSD and those with lymphoma in the validation cohort

Characteristics	AOSD (n=15)	Lymphoma (n=12)	P
Demographics			
Sex			0.057
Female	12 (80.0)	5 (41.7)	
Male	3 (20.0)	7 (58.3)	
Age (years)	33.5±11.9	54.3±16.3	0.001
Disease duration (weeks)	3 (3, 4)	4 (3, 7)	0.106
Clinical manifestation			
Fever >39 ℃	12 (80.0)	5 (41.7)	0.057
Lymphadenopathy	5 (33.3)	11 (91.7)	0.005
Splenomegaly	10 (66.7)	3 (25.0)	0.031
Arthralgia	12 (80.0)	1 (8.3)	<0.001
Pharyngalgia	12 (80.0)	1 (8.3)	<0.001
Rash	13 (86.7)	2 (16.7)	<0.001
Laboratory parameters			
WBC ($\times10^9$/L)	11.5 (10.4, 18.6)	4.7 (3.4, 8.1)	<0.001
Neutrophils (%)	84.0 (73.1, 89.3)	70.4 (63.9, 80.6)	0.010
ESR (mm/h)	71 (46, 86)	64 (28, 78)	0.305
CRP (mg/L)	88.0 (51.0, 177.0)	78.7 (17.8, 97.3)	0.200
Serum ferritin (ng/mL)	3,519 (1,415, 14,751)	960 (244, 3,142)	0.055
LDH (IU/L)	426 (367, 703)	522 (240, 786)	0.938

Categorical variables are presented as number (%) and continuous variables are presented as mean ± SD or median (Q1, Q3). AOSD, adult-onset still's disease; WBC, white blood cell; ESR, erythrocyte sedimentation rate; CRP, C-reactive protein; LDH, lactate dehydrogenase; SD, standard deviation; Q1, first quartile; Q3, third quartile.

Table S2 The ROC curves and the cut-off values of PET/CT parameters

Parameters	AUC	95% CI	P	Cut-off values	95th percentile in healthy controls
SUV_{max} of bone marrow	0.234	0.133–0.336	<0.001	4.4	4.719
SUV_{max} of liver	0.571	0.434–0.709	0.259	3.4	3.997
SUV_{max} of spleen	0.474	0.334–0.614	0.679	5.1	3.078
SUV_{max} of lymph node	0.630	0.501–0.758	0.040	8.3	–
MLV_{total}	0.691	0.576–0.807	0.002	48.42	–
TLG_{total}	0.705	0.594–0.816	0.001	9.0	–

ROC, receiver operating characteristic; PET/CT, positron emission tomography/computer tomography; SUV_{max}, maximum standardized uptake value; MLV, metabolic lesion volume; TLG, total lesion glycolysis.

https://dx.doi.org/10.21037/qims-22-246

Table S3 Univariate logistic regression analysis for differentiating AOSD from lymphoma

Univariate	P	OR	95% CI (lower)	95% CI (upper)
Demographics				
Male gender	<0.001	5.081	2.043	12.636
Age (years)	0.001	1.044	1.017	1.072
Clinical manifestation				
Fever >39 ℃	<0.001	0.064	0.023	0.173
Lymphadenopathy	0.009	22.000	2.180	221.974
Splenomegaly	0.015	2.780	1.221	6.328
Arthralgia	<0.001	0.018	0.005	0.069
Pharyngalgia	<0.001	0.072	0.025	0.209
Rash	<0.001	0.011	0.003	0.046
Laboratory parameters				
WBC ≤10×10^9/L	<0.001	8.744	3.218	23.758
Neutrophils ≤80%	<0.001	11.310	3.606	35.473
Evaluated ESR evaluation	0.002	0.111	0.028	0.437
CRP > ULN	0.068	0.319	0.093	1.088
Ferritin ≤ ULN	0.001	6.493	2.230	18.900
LDH > ULN	0.076	0.415	0.157	1.098
PET/CT parameters				
SUV_{max} of bone marrow <4.7	<0.001	8.228	3.033	22.320
SUV_{max} of LN >8.3	<0.001	4.812	2.025	11.435
MLV_{total} >48.42	<0.001	7.040	2.819	17.578
TLG_{total} >9.0	0.002	7.556	2.114	27.002
SUV_{max} of liver >3.44	0.041	2.368	1.035	5.417
SUV_{max} of spleen >5.1	0.165	1.987	0.753	5.240

AOSD, adult-onset still's disease; WBC, white blood cell; ESR, erythrocyte sedimentation rate; CRP, C-reactive protein; ULN, upper limit of normal; LDH, lactate dehydrogenase; PET/CT, positron emission tomography/computer tomography; SUV_{max}, maximum standardized uptake value; MLV, metabolic lesion volume; TLG, total lesion glycolysis; OR, odds ratio; CI, confidence interval.

https://dx.doi.org/10.21037/qims-22-246

Table S4 PET/CT parameters comparing in different histological type of lymphoma and AOSD

Features	AOSD (n=70)	B (n=19)	T/NK (n=16)	Hodgkin (n=2)	P
Lymph node					
SUV_{max}	4.9 (2.3, 8.0)	11.3 (3.4, 20.4)	8.6 (4.0, 10.7)	(1.0, 16.3)	0.008
Hypermetabolism	70	18	16	2	0.321
MLV_{total} (cm^3)	11.44 (1.57, 39.33)	49.49 (6.85, 93.69)	76.3 (14.2, 214.3)	(1.27, 116.14)	0.001
TLG_{total}	28.1 (2.8, 142.4)	143.6 (21.6, 845.6)	274.1 (38.2, 891.7)	(14.1, 955.9)	<0.001

Data are presented as median (Q1, Q3) or number. PET/CT, positron emission tomography/computer tomography; AOSD, adult-onset still's disease; SUV_{max}, maximum standardized uptake value; MLV, metabolic lesion volume; TLG, total lesion glycolysis; Q1, first quartile; Q3, third quartile.

Table S5 Distribution of model items in the patients with 2 score

Diagnosis	WBC ≤10×10^9/L	Ferritin ≤ ULN	No abnormal bone marrow metabolism	TLG_{total} >9.0
AOSD (n=29)	19 (65.5)	4 (13.8)	13 (44.8)	22 (75.9)
Lymphoma (n=7)	5 (71.4)	1 (14.3)	3 (42.9)	5 (71.4)

Data are presented as number (%). AOSD, adult-onset still's disease; WBC, white blood cell; SUV_{max}, maximum standardized uptake value; ULN, upper limit of normal; TLG, total lesion glycolysis.

https://dx.doi.org/10.21037/qims-22-246